

Water Flow in Carbon Nanotubes: Transition to Subcontinuum Transport

John A. Thomas and Alan J. H. McGaughey*

Department of Mechanical Engineering, Carnegie Mellon University, Pittsburgh, Pennsylvania 15213, USA

(Received 23 December 2008; published 8 May 2009)

The structure and flow of water inside 75 and 150 nm-long carbon nanotubes with diameters ranging from 0.83 to 1.66 nm are examined using molecular dynamics simulation. The flow rate enhancement, defined as the ratio of the observed flow rate to that predicted from the no-slip Poiseuille relation, is calculated for each tube and the liquid structure is examined using an axial distribution function. The relationship between the intermolecular water structure and water flow is quantified and differences between continuum and subcontinuum flow are discussed.

DOI: 10.1103/PhysRevLett.102.184502

PACS numbers: 47.56.+r, 47.61.-k, 61.20.Ja

An important step towards understanding liquid flow in nanoscale systems is to predict the transition from continuum to subcontinuum transport as the flow area decreases. In a continuum system, the behavior of a liquid can be described in terms of infinitesimal volumetric elements that are small compared to the flow domain but have well-defined thermophysical properties. Applying Newton's second law to a system of volumetric elements gives rise to the Cauchy and Navier-Stokes equations, which can be used to derive the Poiseuille and other continuum-level flow relations [1]. In a system where the size of a liquid molecule is comparable to the size of the flow domain, however, the notion of a representative volumetric element is invalid and the applicability of continuum-based relations is questionable. Within such "subcontinuum" systems, the movement of individual molecules must be considered when predicting mass and momentum transport [2].

In this Letter, we use molecular dynamics (MD) simulation to examine pressure-driven water flow through carbon nanotubes (CNTs) with diameters ranging from 0.83 to 1.66 nm, where a transition from continuum to subcontinuum flow with decreasing CNT diameter is expected [3,4]. We examine flow through 75 and 150 nm-long CNTs, which are much longer than the 1–3 nm-long CNTs examined in a previous investigation [4]. We begin by quantifying the relationship between pressure gradient and average flow velocity for each CNT and then identify the transition to subcontinuum water flow. Next, we predict the liquid structure inside each CNT and correlate the structure to molecular transport. For subcontinuum systems we find that the liquid structure relaxation time, which we define as the time required for a water molecule to become uncorrelated from an initial structural arrangement, exceeds a time scale characteristic of the flow. This behavior leads to coordinated molecular transport inside the CNT and a nonmonotonic relationship between CNT diameter and average flow velocity. We find that the water structure is long-ranged, and discuss how the relationship between

pressure gradient and flow velocity will depend on tube length for CNT fragments shorter than 10 nm.

The average flow velocity \bar{v} of an incompressible, creeping liquid (Reynolds number much less than one) inside a tube with a uniform cross-sectional area is given by the Darcy law, $\bar{v} = \gamma(\frac{\Delta P}{L})$, where ΔP is the pressure difference across the tube, L is its length, and γ is the hydraulic conductivity [1]. Although the Darcy law is an empirical expression, the hydraulic conductivity of a Newtonian liquid in a circular tube subject to the no-slip boundary condition, $\gamma_{\text{no-slip}}$, can be found directly from the no-slip Poiseuille relation, $\gamma_{\text{no-slip}} = \frac{D^2}{32\mu}$, where D is the tube diameter and μ is the liquid viscosity [3].

Liquid slip at the solid-liquid boundary, confinement-induced reductions in the liquid viscosity, and subcontinuum changes to the liquid structure can all cause the actual hydraulic conductivity (γ_{actual} , as measured from experiment or predicted from MD simulation) to exceed that calculated from the Poiseuille relation [2]. This increase in γ has led to the definition of a flow enhancement factor, ε , given by $\varepsilon = \gamma_{\text{actual}}/\gamma_{\text{no-slip}}$ [3]. For CNTs with diameters larger than 1.6 nm, the variation in ε with CNT diameter can be understood in terms of slip at the water-CNT boundary and diameter-related changes to the water viscosity [3]. In CNTs with smaller diameters, however, water molecules have been shown to assemble into diameter-dependent one-dimensional structures for which neither the slip length nor the effective viscosity is well defined [2]. This confinement-induced change to the liquid structure necessitates a subcontinuum description of the liquid [5,6].

We simulate pressure-driven water flow through 0.83, 0.97, 1.10, 1.25, 1.39, and 1.66 nm-diameter single-walled armchair CNTs. A snapshot from a typical simulation, which consists of a water-filled CNT fragment connected to two water-filled reservoirs, is presented in Fig. 1. All simulations are performed in the *NVT* ensemble (constant number of particles, volume, and temperature) at a temperature of 298 K and flow is driven by a reflecting particle

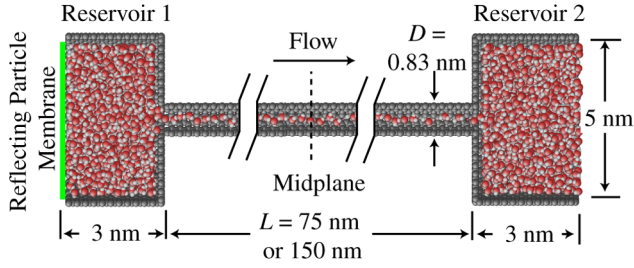


FIG. 1 (color online). Snapshot from a typical flow simulation for the 0.83 nm-diameter CNT. A constant pressure difference is established between the reservoirs using a reflecting particle membrane. After a 0.25 ns initialization period, the mean pressure in each reservoir remains constant over the duration of the ensuing data collection period and flow through the tube is steady. Periodic boundary conditions are imposed in the flow direction. The number of molecules inside the CNT ranges from 310 ± 5 for the 75 nm-long, 0.83 nm-diameter CNT to 3676 ± 20 for the 150 nm-long, 1.66 nm-diameter CNT.

membrane placed between the reservoirs [7]. We use the TIP5P potential to model interactions between water molecules [8], the Lennard-Jones potential of Werder *et al.* to model the interactions between water molecules and carbon atoms [9], and keep the carbon atoms fixed. We maintain the temperature of the system by applying a Berendsen thermostat to the velocity components transverse to the flow direction [10]. We note that applying the thermostat to all three directions does not affect the flow predictions.

We find that fixing the carbon atoms has no effect on the structure of water molecules inside the CNT. The number of molecules in the system is chosen such that the water density in the reservoirs is 1000 kg/m^3 and the average number of water molecules in the CNT fragment is constant. As presented in Fig. 2(a), the CNT diameters examined here have water structures corresponding to single-file molecular chains (0.83 nm), tilted pentagonal rings (0.97 nm), stacked pentagonal rings (1.10 nm), stacked hexagonal rings (1.25 nm), and disordered bulklike water (1.39 and 1.66 nm). The water structure and density we predict for each CNT are unaffected by flow and consistent with previous MD simulation results [11].

In Fig. 3(a), we plot \bar{v} vs $\Delta P/L$ for the 75 nm-long CNTs. Each point in Fig. 3(a) is the average of at least four independent 1 ns simulations. Consistent with the Darcy law, the average flow velocity for each CNT increases with increasing pressure gradient. For a fixed value of $\Delta P/L$, however, the average flow velocity does not increase monotonically with CNT diameter, as would be predicted from the Poiseuille relation. Instead, when subject to the same pressure gradient, the average velocity decreases from the 0.83 nm CNT to the 1.10 nm CNT, is similar in the 1.10 and 1.25 nm CNTs, and then increases from the 1.25 nm CNT to the 1.66 nm CNT.

The nonlinear relationship between \bar{v} and $\Delta P/L$ is the result of inertial losses (i.e., minor losses) at the two CNT-reservoir boundaries. Inertial losses are velocity-dependent

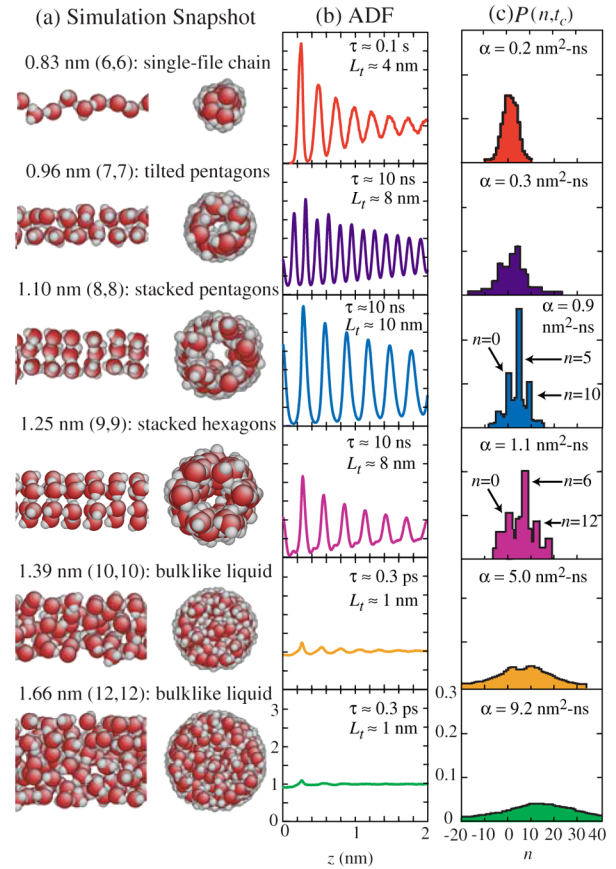


FIG. 2 (color online). (a) Water structures inside the 0.83–1.66 nm-diameter CNTs. Carbon atoms are removed for clarity and the chirality vector for each CNT is provided. (b) Axial distribution function (ADF), structure relaxation time τ , and extent of the ADF, L_t , for each CNT. (c) $P(n, t_c)$, the probability that n molecules cross the system midplane over the characteristic flow time t_c . The CNT permeability α is provided for $\Delta P/L = 4 \times 10^{14} \text{ Pa/m}$.

and caused by sudden expansions, contractions, and other obstacles in the flow field. The penalty associated with such losses, $\Delta P_m(\bar{v})$, can be incorporated into the Darcy law: $\bar{v} = \gamma \left[\frac{\Delta P - \Delta P_m(\bar{v})}{L} \right]$ [1]. Given that the inertial losses are unknown, the hydraulic conductivity can be extracted from this modified form of the Darcy law as follows: Consider a long CNT with length L_l , and a shorter CNT with length L_s , with identical diameters and connected to identical reservoirs. Let the ratio of length to diameter for both tubes be large such that the entrance and exit effects are decoupled. If both systems have the same average flow velocity, the inertial losses in each system will be the same. However, due to additional frictional flow resistance in the longer CNT, the total pressure drop across it, ΔP_l , will exceed that across the short CNT, ΔP_s . Applying the modified Darcy law to both systems and eliminating $\Delta P_m(\bar{v})$ gives $\gamma = \bar{v}[(L_l - L_s)/(\Delta P_l - \Delta P_s)]$. For the 1.66 nm-diameter CNT, the hydraulic conductivity calculated for the systems investigated here is within 17% of the value we predicted in our previous work, which was free of

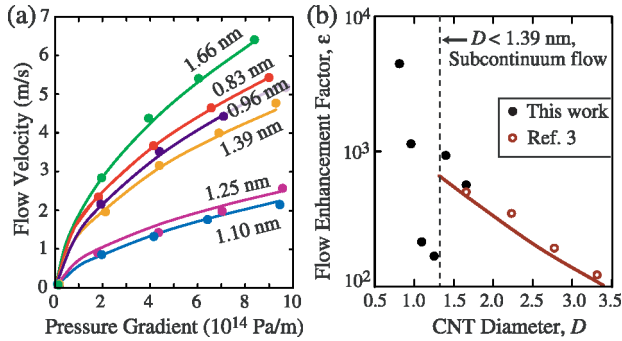


FIG. 3 (color online). (a) Relationship between average flow velocity \bar{v} and applied pressure gradient $\Delta P/L$ for the 75 nm-long CNTs. A similar relationship exists for the 150 nm-long CNTs. We note that \bar{v} is well below the molecular thermal velocity (340 m/s at $T = 298$ K). For each data point, the standard deviation in \bar{v} and $\Delta P/L$ is 0.5 m/s and 2×10^{13} Pa/m, leading to a $\pm 25\%$ uncertainty in ϵ . Guide lines are added to highlight the trends. (b) Variation in flow enhancement factor ϵ with CNT diameter D . The dashed line between $D = 1.25$ nm and $D = 1.39$ nm delineates continuum and subcontinuum flow regimes. The line in the continuum regime is a model we developed previously [3].

reservoirs and had no inertial losses. We estimate the uncertainty in γ (and thus ϵ) to be $\pm 25\%$ from the measured variances in \bar{v} and $\Delta P_l - \Delta P_s$. We find that, within this prediction uncertainty, γ is invariant over the flow velocities considered for a given CNT diameter.

In Fig. 3(b), we present the variation of ϵ with CNT diameter. We also include the enhancement values for the 1.66–to 3.33 nm-diameter CNTs we reported previously [3]. In CNTs with diameters larger than 1.66 nm, where a continuum description of water flow is valid, we found that ϵ increased monotonically with decreasing CNT diameter. Here, we find that this trend extends to the 1.39 nm-diameter CNT. The abrupt reduction in flow enhancement between the 1.39 and 1.25 nm-diameter CNTs suggests a transition to subcontinuum transport, which is consistent with the change from disordered bulklike water to one-dimensional structures with decreasing CNT diameter [see Fig. 2(a)]. The variation in flow enhancement within CNTs with diameters smaller than 1.25 nm cannot be described using continuum relations and, as we will show, is related to the water structure.

In Fig. 2(c), we provide the molecular permeability α of each CNT corresponding to a pressure gradient of 4×10^{14} Pa/m. Despite the decrease in flow velocity from the 0.83 to the 1.10 nm-diameter CNT, the permeability (which incorporates the effects of diameter-related changes to the flow area, water density, and velocity) increases monotonically with CNT diameter for all tubes. This trend arises from the fact that the cross-sectional flow area increases faster with diameter than the structure-related reductions in the flow velocity.

To quantify the variation in liquid structure with tube diameter, in Fig. 2(b) we present the axial distribution

function (ADF) for water molecules inside each CNT. We define the ADF, $a(z)$, by $\int_{z=0}^{z=\pm L} a(z) \frac{\pi D^2}{4} dz = N_t - 1 \approx N_t$, where N_t is the number of water molecules between $z = \pm L$. In CNTs with diameters greater than 1.66 nm, the ADF has a small peak at $z = 0.3$ nm and is invariant with CNT diameter. The position of this peak is similar to the position of the first peak in the radial distribution function of bulk water. The ADF inside the 1.39 nm-diameter CNT is comparable to that of larger tubes, suggesting that confinement-induced changes to the liquid structure are insignificant in this CNT [12]. Inside the 1.25–0.83 nm-diameter CNTs, where the layered and single-file molecular structures are present, the axial positions of the water molecules are strongly correlated and oscillations in the ADF extend 4–10 nm from the origin molecule. Such long-range positional correlation, which is not present in bulk water, is a distinguishing feature of subcontinuum liquids [2]. We find no difference between the ADFs in the 75 and 150 nm-long CNTs.

In CNTs with diameters less than 1.39 nm and lengths shorter than about 10 nm, all the water molecules inside the tube will have correlated positions. Although the distinction between solid phase water and liquid phase water is unclear for such systems, we expect that the solidlike molecular structure will limit the mobility of individual molecules and lower the average flow velocity of water inside such short CNTs. This hypothesis is supported by the MD simulation data of Corry [4], who investigated pressure-driven water flow through CNT membranes with diameters similar to those investigated here, but with lengths of 1.3 and 2.6 nm. The positions and movement of water molecules inside the short CNTs were indeed correlated, and transport through the tubes occurred via collective bursts. Moreover, the flow enhancement factors we calculate from the Corry data are 1–10, a range lower than the 100–1000 range we predict here for 75 and 150 nm-long CNTs. This result suggests that as the CNT length decreases below 10 nm and the molecules at the tube inlet become increasingly coupled to those at the tube outlet, mass transport will become less like flow through a pipe and more like coordinated diffusion through a two-dimensional pore. This transition will reduce the flow rate through the tube and cause a reduction in the flow enhancement factor.

Although the CNTs investigated here are longer than the oscillations in their ADFs, the local liquid structure in each tube still governs the molecular transport through it. This coupling between structure and flow can be elucidated by examining the cumulative midplane mass flux $n(t)$. In Fig. 2(c), we present the probability $P(n, t_c)$ that n molecules cross the CNT midplane over a characteristic flow time t_c . We define t_c from $t_c = \frac{L_c}{\bar{v}}$, where L_c is a characteristic length scale. We set L_c equal to the location of the first peak in the ADF and calculate $P(n, t_c)$ for each flow simulation. Since the liquid structure does not vary with flow velocity (over the range considered here), $P(n, t_c)$ for

each CNT collapses onto a velocity-independent distribution. We note that with $L_c \sim 0.17\text{--}0.3$ nm and $\bar{v} \sim 1\text{--}7$ m/s, t_c is $O(100)$ ps.

Inside the 1.66 nm-diameter CNT (where flow can be modeled using continuum-based relations) $P(n, t_c)$ is non-zero over a large range of n . This large range is accessible because the structure relaxation time, which we estimate to be 0.3 ps from the decay of the velocity autocorrelation function, is very small compared to t_c . The flow is therefore independent of liquid structure and a random number of molecules, subject to the distribution of $P(n, t_c)$, can cross the midplane during t_c . Although the accessible range of n increases with CNT diameter, we find that the shape of the $P(n, t_c)$ distribution in larger CNTs is similar to what we report here for the 1.66 nm diameter tube and find no appreciable change in the structure relaxation time. This smooth distribution of $P(n, t_c)$ is also present in the 1.39 nm-diameter CNT, further suggesting that the flow in this tube is independent of structure and a continuum description of mass flow will be appropriate.

Inside the 1.25 nm-diameter CNT, $P(n, t_c)$ exhibits peaks at $n = 6$ and 12. A similar distribution is present inside the 1.10 nm-diameter CNT, where $P(n, t_c)$ exhibits peaks at $n = 5$ and 10. These peaks, which are related to the stacked hexagonal and pentagonal rings in the tubes, indicate a coupling between structure and flow. The relaxation time of the layered water structure inside these CNTs, as estimated from MD simulation, is $O(10)$ ns [5,6], indicating that water molecules may travel from the tube inlet to the tube outlet as members of a single layer. Unlike bulklike systems, where water molecules can move independently, the transport of molecules in these structured subcontinuum systems is conditional upon the movement of nearby layers. A layer of water molecules that fills an energetically stable CNT surface site can therefore impede the movement of other layers. Such localized limitations on transport will reduce \bar{v} and lower the overall flow enhancement (see Fig. 3). This hypothesis is consistent with the findings of Mamontov *et al.*, who demonstrate from neutron scattering experiments and MD simulation that the water molecules in layered structures have, on average, less mobility than the molecules in bulklike water [12].

Between the 1.10 and 0.83 nm-diameter CNTs, the liquid structure transitions from stacked pentagonal rings to tilted pentagonal rings and finally to a single-file molecular chain. With decreasing CNT diameter, we find that the effects of layer-by-layer transport become less prominent, the spatial extent of the ADF decreases [see Fig. 2(b)], and the average flow velocity increases for a given pressure gradient [see Fig. 3(a)]. Although the mass transport mechanisms within these tubes are not yet clear, in a previous work we found that water molecules become less coupled to the CNT surface with decreasing CNT

diameter [3]. This effect will reduce flow friction in smaller CNTs and may contribute to the increase in flow velocity with decreasing diameter. In the 0.83 nm-diameter CNT, where the single-file water structure relaxation time has been estimated to be $O(0.1)$ s [13], the probability of two or more molecules crossing the midplane in either the positive or negative direction is 0.6. This behavior is the result of coordinated molecular motion inside the CNT. It confirms that, although the tube inlet and tube outlet are decoupled in our system, localized bursting still governs mass transport inside long-length, small-diameter CNTs.

Although this work is focused on water flow through CNTs, several trends can be extrapolated to the more general field of subcontinuum liquid transport. First, unlike predictions from continuum mechanics, the flow enhancement in subcontinuum systems may not increase monotonically with decreasing flow area. Instead, when the flow area is comparable to the size of the liquid molecules, confinement-induced changes to the liquid structure may reduce the flow enhancement and must be considered. Second, if the system length is comparable to the correlation length, the liquid inlet and outlet are not independent and the hydraulic conductivity may depend on system length. Within short systems, transport may therefore be less like flow through a pipe and more like coordinated diffusion through a two-dimensional pore. Third, liquid structure and liquid flow are independent in systems where the characteristic flow time scale is much longer than the structure relaxation time. These scales must be considered when comparing results from different flow investigations and examining flow-structure interactions.

*mcgaughey@cmu.edu

- [1] J. Bear, *Dynamics of Fluids in Porous Media* (American Elsevier, New York 1972).
- [2] H. Verweij *et al.*, *Small* **3**, 1996 (2007).
- [3] J. A. Thomas and A. J. H. McGaughey, *Nano Lett.* **8**, 2788 (2008).
- [4] B. Corry, *J. Phys. Chem. B* **112**, 1427 (2008).
- [5] S. Joseph and N. R. Aluru, *Phys. Rev. Lett.* **101**, 064502 (2008).
- [6] A. Striolo, *Nano Lett.* **6**, 633 (2006).
- [7] J. Li *et al.*, *Phys. Rev. E* **57**, 7259 (1998).
- [8] M. W. Mahoney and W. L. Jorgensen, *J. Chem. Phys.* **112**, 8910 (2000).
- [9] T. Werder *et al.*, *J. Phys. Chem. B* **107**, 1345 (2003).
- [10] H. J. C. Berendsen *et al.*, *J. Chem. Phys.* **81**, 3684 (1984).
- [11] A. Alexiadis and S. Kassinos, *Chem. Rev.* **108**, 5014 (2008).
- [12] E. Mamontov *et al.*, *J. Chem. Phys.* **124**, 194703 (2006).
- [13] J. K. G. Hummer and C. Dellago, *Proc. Natl. Acad. Sci. U.S.A.* **105**, 13 218 (2008).